Modeling the Austenite Ferrite Transformation by Cellular Automaton

Improving Interface Stability

M.M. Mul

TUDelft
Delft
University of
Technology

Modeling the Austenite Ferrite Transformation by Cellular Automaton
Improving Interface Stability

MASTER OF SCIENCE THESIS

For the degree of Master of Science in Applied Mathematics at Delft University of Technology

M.M. Mul

September 18, 2014

Faculty of Electrical Engineering, **Mathematics** & Computer Science (EEMCS) · Delft University of Technology

Abstract

A three-dimensional mixed-mode cellular automaton model [C. Bos, M. G. Mecozzi, and J. Sietsma. Computational Materials Science 48.3 (2010): 692-699] for the austenite to ferrite transformation in low-carbon steel has been analyzed and improved. A comparison between the new and conventional model has been made and the improvements found are significant. Interface velocity is based on diffusion of carbon atoms and determined by the local density of carbon. A higher grain boundary carbon diffusion coefficient is applied. The conventional model has been revised and stabilized. Real dilatometry tests have been used to mirror the transformation behaviour of the model with reality. For a one-dimensional model it has been shown that the space-discretizing cellular automaton model converges to the space-continuous method of Murray-Landis.

Table of Contents

List of Figures

List of Tables

Acknowledgements

This thesis would not have been possible without the support of many people. First of all, I would like to acknowledge my supervisor Dr.ir. F.J. Vermolen for his assistance during this thesis work. The ideas and talks during our appointments were always inspiring and motivating, especially the ones when he said to me, "I know you don't like the writing part so much, but it is very necessary that you do it". I would also like to thank my daily supervisor at Tata Steel, Dr.ir. C. Bos, for his clear guidance throughout the process and his support whenever I needed it. Thank you both for the great communication and cooperation during this work. I thank Prof.dr.ir. C Vuik for recommending me the awesome Erasmus Mundus COSSE programme. Then, of course, I should not forget to show gratitute to my sponsors from Deventer. Without your financial and moral support I would not have been able to deliver this thesis. For the moral support, but also for the many evenings that dinner waited at home, I would like to thank Mathilde. Without you, my free evenings would have involved a whole lot more of cooking.

Delft, University of Technology   M.M. Mul
September 18, 2014

"Don't drink too much, but also don't drink too little."

— *Fred Vermolen*

Chapter 1

Introduction

Steel production plays an important role in the development of our society. Construction, transport and packaging are three sectors which would not exist in their current state if steel production had not been continually improving over time. As a result, manufacturers have some freedom in steel properties. The automotive industry uses different steels for various car parts in order to make their cars lighter or stronger. Developing and understanding the steel production process will contribute to the further evolution of our society. Typically, steel is made by melting iron ore with cokes, resulting in a liquid carbon-rich steel. Then, oxygen is added which reacts with carbon to reduce the amount of carbon in the molten steel. Since this process is exotherm, scrap metal is added to control the temperature of the liquid. At this point, other elements can be added in an attempt to change final mechanical properties. The next step consists of casting the liquid into solid blocks. These blocks of steel are hot or cold rolled into metal sheets, which is an end product of the steel producer, see Figure 1-1. Since solid steel has two different atom lattices, depending on its temperature, the transformation between these lattices is of interest while researching steel properties at room temperature. After all, the final properties of steel depend on the whole process during steel production, starting from the possible impure resources iron ore and coal and ending with the final cooldown to room temperature. The phase transformation between austenite and ferrite occurs in the region between 1000 K and 1185 K. This is the result of iron atoms preferring a different iron atom lattice over the other.

The austenite to ferrite transformation process can be identified as a moving boundary problem. There exist several methods to deal with this type of problem. Front-capturing methods are very suited for moving boundary problems where topological changes occur, which is the case when ferrite starts to nucleate in the austenite structure. Phase field and level set methods are front-capturing methods and are widely used to research phase transformations[1, 2]. The phase field method introduces a diffusive interface, where the phase transformation occurs, and avoids direct implementation of the interface conditions. The level set method makes it easy to follow the contours of transforming topological objects and is also highly suitable for the phase transformation problem. Another widely used method is cellular automaton [3, 4, 5, 6, 7, 8, 9, 10, 11, 12, 13] which divides the domain into a regular grid of

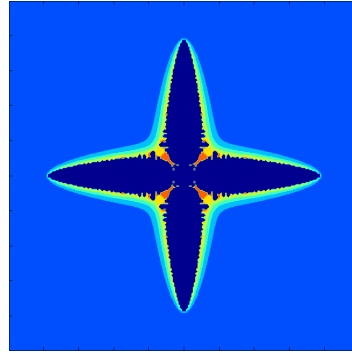**Figure 1-1:** The end product of a steel manufacturer.

Figure 1-2: An example of a dendrite originated from a model designed for ferrite grain growth.

cells which transform due to a transformation rule. This report focuses on improving cellular automaton to model phase transformations. In current cellular automaton implementations of this problem, dendritic growth patterns have been observed, see Figure 1-2. In solidification of steel this behaviour is physically natural, however, during the phase transformation that happens when steel is cooled down these patterns are not observed. Efforts are made to reduce and possibly avoid dendritic growth completely.

There exist at least three good reasons to motivate the work on improving this type of transformation models. Firstly, modeling the austenite to ferrite transformation in a more accurate way may contribute to the reduction of physical experiments. Secondly, analyzing the microstructure of a model is more convenient than microscopic research on steel samples. Thirdly, the amount of experiments can be highly increased, which results in a higher rate of feedback and therefore a possible faster development of new types of steel or different heat treatments.

The first Chapter is about the models which are used for the transformation simulations. First, an outline of test problem for examining the unwanted behaviour of dendritic growth will be given. Then, a more sophisticated model is explained to cover the transformation from a structure of austenite grains to a mixed ferrite austenite grain structure. The moving boundary problem will then be subjected by Cellular Automaton, which results in new submodels for interface growth and carbon dynamics. This thesis then proceeds by reporting on the methods that are used to turn the model into computing algorithms. A carbon smoothing approach is described with the aim of suppressing dendritic growth behaviour. A complete overview of an algorithm is given to encourage reproduction. Results of findings of model behaviour are presented in a visual way for clear understanding. The results and implementation of the model are discussed, especially the dendritic growth behaviour. As a conclusion one could say that modeling the austenite to ferrite transformation by Cellular Automaton has been enhanced and diffusion-based transformation models are now operational.

Chapter 2

The Model

The austenite to ferrite transformation is a complex process on micro scale of moving iron atoms inside a solid material. First, the mechanics of this process will be described. Initially, it is assumed that there is a structure of austenitic grains within a domain of constant temperature. The orientation of the atom lattices differ from grain to grain, which results in impurities at the edges of these grains. Furthermore, it is assumed that a certain amount of carbon is present in the domain. The process starts, when the temperature is quickly altered to a constant lower temperature everywhere in the domain. The result of this temperature change is that the preferred iron atom lattice changed from austenite to ferrite. From this moment the transformation starts by the nucleation of ferrite grains within the austenitic structure. The corners and edges of austenite grains are assumed to be the most likely nucleation points of ferrite in the domain. Inside the ferrite grains there is less space for carbon atoms and therefore it is pushed in front of the ferrite interface into the austenite. Due to lower temperatures, ferrite grains are expanding over time. However, the higher concentration of carbon at its own interface results in a slow-down of transformation. This means that the ferrite grains need to wait a little until carbon atoms are dissolved into the austenitic domain. Thus, the velocity of the moving interface depends heavily on the local carbon concentration[7]. It is assumed that the expansion of ferrite is faster at austenite-austenite interfaces, because there the iron atom are less structured into lattices. When the ferrite growth causes the austenitic grains to be saturated with carbon atoms, the process has reached equilibrium.

The phase transformation from austenite to ferrite will be modeled using cellular automaton, because CA is advantageous in its simplicity versus phase field[14] or level set methods[2]. The CA recrystallization model from Bos et al.[8] is available and could be improved at some points. Thus, from a pragmatic point of view it is wise to continue with this type of model. Further, other transformations, recrystallization and nucleation processes are present in this model. The submodel for determining the carbon interface concentration based on an assumed exponential profile will be replaced by solving the carbon concentration using a finite difference grid on the austenite domain, because it is suspected that the exponential carbon profile model is not accurate in the multi-grain model.

2-1   Single-grain Test Model

The fundamental test problem that will be investigated is the austenite to ferrite phase transformation. This is a concentration-based moving boundary problem. The interface S between the ferrite domain Ω^α and the austenite domain Ω^γ is the main interest, see Figure 2-1. For the whole domain $\Omega = \Omega^\alpha \cup \Omega^\gamma$ the n-dimensional cube with edges of length L is used. For dimension n up to 3, the domain is $\Omega = [0, L]^n$. The magnitude of L is of the order 10^{-6} m. The test problem will be further specified by initial conditions and boundary conditions.
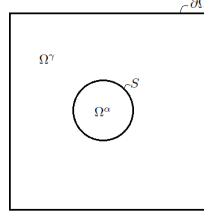

Figure 2-1: Domain of the moving boundary problem in $\mathbb{R}^2$.

Initial conditions: The initial state is a domain consisting of austenite with a small grain of ferrite situated within the austenite.

Boundary conditions: The diffusion of carbon in austenite requires boundary conditions. The boundary of Ω^γ is $\partial\Omega^\gamma = \partial\Omega \cup S$. The size of the domain for simulating microstructural changes in steel is restricted due to computation times. Since only a small part of the steel is simulated, boundary conditions with symmetric behaviour are chosen. Using Neumann boundary conditions on all sides of the domain, implicitly it is assumed that the microstructural development in time is mirrored on all sides outside the domain. The assumption of constant concentration of carbon in ferrite results in a flux of carbon into the austenite domain, depending on the velocity of the interface v_n. This gives us our boundary condition on S.

The moving boundary problem can be stated as the following system.

$$
\begin{cases}
v_n & = \ M\Delta G(x_s^\gamma) & \text{the normal velocity of } S, \\
\frac{\partial x}{\partial t} & = \ \nabla \cdot (D(x,z)\nabla x) & \text{in } \Omega^\gamma, \qquad t > 0, \\
\frac{\partial x}{\partial n} & = \ 0 & \text{on } \partial\Omega, \\
\frac{\partial x}{\partial n} & = \ -(x_s^\gamma - x^\alpha)v_n & \text{on } S, \\
x(t = 0) & = \ x_0.
\end{cases}
\tag{2-1}
$$

In this system, x is the carbon concentration, M the interface mobility, ΔG the driving force, $D(x)$ the diffusion coefficient, x_s^γ the carbon concentration at the interface S, x^α the equilibrium carbon concentration in ferrite and finally x_0 the initial carbon distribution. Remark that the diffusion coeffcient $D(x, z)$ may depend on the carbon concentration x or the location in the domain. Some models assume otherwise to simplify the problem, but experiments show that D really is carbon dependent, see Ågren[15].

2-2 Multi-grain Model

The model covered by this work of the austenite to ferrite phase transformation is decribed in this section. It is similar to the single grain test model, but the austenite and ferrite structure is added. Based on experiments, it is assumed that the initial structure of austenitic grains are a Voronoi structure. The austenite grains are written as A_i for $i = 1...N_A$, where N_A is the total number of grains. Ferrite grains F_i with total number of grains N_F are defined analogously. The interface S between the ferrite domain $\Omega^\alpha = \cup_{i=1}^{N_F} F_i$ and the austenite domain $\Omega^\gamma = \cup_{i=1}^{N_A} A_i$ is defined as

$$S = \bigcup_{i=1}^{N_F} \bigcup_{j=1}^{N_A} \partial F_i \cap \partial A_j, \tag{2-2}$$

where ∂F_i and ∂A_j are the boundary of the domain of ferrite and austenite grain i and j, respectively. For the whole domain $\Omega = \Omega^\alpha \cup \Omega^\gamma$ the n-dimensional cube with edges of length L is used. An example of such a domain in two dimensions is given by Figure 2-2. For dimension n up to 3, the domain is $\Omega = [0, L]^n$. The test problem will be further specified by initial conditions and boundary conditions.

Figure 2-2: Schematic example of an austenitic structure with growing ferrite grains in $\mathbb{R}^2$.

Initial conditions: The initial state is a domain consisting of austenite grains in a Voronoi structure with a number N_F of ferrite nuclei that start to grow. This model for ferrite nucleation is called *site saturation*.

Boundary conditions: In this model periodic boundary conditions are used, which is a common technique for this type of problem[8].

The moving boundary problem can be stated as the following system.

$$\begin{cases} v_n & = & M\Delta G(x_s^\gamma) & \text{the normal velocity of } S, \\ \frac{\partial x}{\partial t} & = & \nabla \cdot (D(x)\nabla x) & \text{in } \Omega^\gamma, \quad t > 0, \\ \frac{\partial x}{\partial n} & = & 0 & \text{on } \partial\Omega, \\ \frac{\partial x}{\partial n} & = & -(x_s^\gamma - x^\alpha)v_n & \text{on } S, \\ x(t = 0, z) & = & x_0(z). \end{cases} \tag{2-3}$$

In this system, x is the carbon concentration, M the interface mobility, ΔG the driving force, $D(x)$ the diffusion coeffcient, x_s^γ the carbon concentration at the interface S, x^α the equilibrium carbon concentration in ferrite and finally x_0 the initial carbon distribution. The diffusion coefficient $D(x, z)$ may depend on the carbon concentration x and the location in space z. For the model it is assumed that the diffusion coefficient is higher at grain interfaces and therefore the coefficient is simplified to $D(z)$.

2-3   Cellular Automaton

A popular approach for modeling the austenite to ferrite transformation is Cellular Automaton(CA), which appears in many articles[3, 16, 4, 5, 17, 6, 18]. An introductory review of using CA for this type of problem can be found in a paper written by K.G.F. Janssens[3]. A Cellular Automaton is a discrete model with a regular grid of cells. Each cell has a set of properties, most importantly its state, neighbourhood, and transformation rule. The state represents to which type of grain the cells belong. Given an initial state, each time step the state of a cell is updated by a rule that is a mathematical function of the states of its neighbours.

Grids   Any regular grid is allowed in CA models. The most common regular grid is built from squares. But also other grids are used, see Figure 2-3. Hexagonal grids are sometimes used to reduce grid anisotropies[9, 11].

Figure 2-3: Square grid(l), triangular grid(m), and hexagonal grid(r)

Neighborhoods   Two types of neighborhoods will be defined, the Von Neumann neighborhood and the Moore neighborhood. The neighborhood of a cell is usually defined as a set of cells around it, including itself. Using lexicographic numbering on a square $n \times n$ grid, the Von Neumann neighborhood of cell i is defined as the collection of cells

$$\mathcal{N}_i = \{\text{Cells } j : j \in \{i - 1, i, i + 1, i - n, i + n\}\}. \tag{2-4}$$

The 3×3 Moore neighborhood of cell i is defined as the collection of cells

$$\mathcal{M}_i = \{\text{Cells } j : j \in \{i + n - 1, i + n, i + n + 1, i - 1, i, i + 1, i - n - 1, i - n, i - n + 1\}\}. \tag{2-5}$$

Figure 2-4 illustrates these two definitions.

In general, the $m \times m$ Moore neighbourhood of a cell i consists of all cells within an $m \times m$ cube of cells around i.

Figure 2-4: Two-dimensional Von Neumann neighborhood(l) and 3×3 Moore neighborhood(r)

2-3-1 The Framework

To model ferrite grain growth, a 3-dimensional Cellular Automaton model with carbon diffusion is constructed. This model is based on existing models from literature, e.g. in Bos et al. [8]. Consider a cubic domain Ω with n cells of length Δz on each side. Using periodic boundaries, all cells have 26 neighbours that can be divided into three different types based on the Euclidian distances measured from the cell centres. In general a k-nearest neighbour is defined as a neighbour whose center lies at a distance of $d(k)$ from the reference cell.

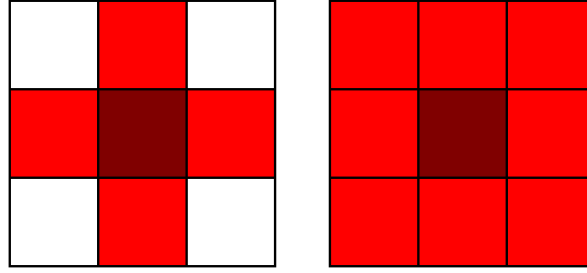|	Distance	Informal notation
$d(1)$	Δz	*Nearest* Neighbour
$d(2)$	$\sqrt{2}\Delta z$	*NextNearest* Neighbour
$d(3)$	$\sqrt{3}\Delta z$	*NextNextNearest* Neighbour

Table 2-1: k-nearest neighbours

For each cell i its binary state is defined as $\zeta_i \in \{0, 1\}$. The ferrite and austenite domains in problem (2-3) are defined as collections of cells,

$$
\begin{aligned}
\Omega^\alpha &= \{\text{Cells } i : \zeta_i = 1\} \\
\Omega^\gamma &= \{\text{Cells } i : \zeta_i = 0\}
\end{aligned}
\tag{2-6}
$$

The most important cell properties are outlined in table 2-2.

Description	Symbol	Defined for
Average carbon concentration at the interface	x_s	Ferrite interface cells
Growth velocity	v	Ferrite interface cells
Outward growth length	ℓ	Ferrite interface cells
Inward growth length	λ	Austenite interface cells
Carbon concentration	x	All cells

Table 2-2: Cell properties

Interface Growth Dynamics

For each ferrite interface cell, the growth length $\ell(t)$ is defined as

$$\ell(t) = \int_{t_0}^{t} v_n(\tau) \, \mathrm{d}\tau, \tag{2-7}$$

where $v_n(t)$ is the outward normal growth velocity of the interface S and $t_0 = \inf\{t : v_n(t) > 0\}$. This growth length can be interpreted as the radius of a growing ball with radius ℓ centered in the cell. This omnidirectional growth model is a simplification making the consideration for different growth velocites for every direction obsolete. The growth velocity v_n is computed by a model for the interface velocity in the outward normal direction from the ferrite phase α, which can be formulated as

$$v_n = M_0 \cdot e^{\frac{-Q^{\alpha,\gamma}}{RT}} \Delta G(T, x_s), \tag{2-8}$$

where M_0 and $Q^{\alpha,\gamma}$ are respectively the pre-exponential factor and the activation energy for the interface mobility. Additionally, R is the gas constant and T the temperature. The driving force ΔG is assumed to be a function of the temperature T and the carbon interface concentration x_s. Using the software Thermo-Calc® this function can be extracted for the desired steel alloy. Using a transformation method based on the growth length ℓ, cells are transformed from austenite to ferrite. If fast growth on grain boundaries needs to be modeled, it is possible to multiply $Q^{\alpha,\gamma}$ by some factor between 0 and 1.

Carbon Dynamics

Contrary to the more simplistic assumption of an exponential profile[19], the carbon concentration will be computed by the diffusion equation. First, the use of atomic fraction as a concentration in the diffusion equation is justified. Let

$$f_C = \frac{a_C}{a_C + a_{Fe}} \tag{2-9}$$

be the fraction of carbon atoms of a cell with volume $V = (\Delta z)^2$. Since low-carbon steel is considered, it is assumed that the number of carbon atoms is much smaller than the number of iron atoms, i.e. $a_C \ll a_{Fe}$. Furthermore, it is assumed that a_{Fe} per cell is constant, i.e. density variations of iron atoms are neglected. In reality, these variations are small[20]. Inserting these two assumptions, the following relationship is obtained

$$\frac{f_C}{V} \approx \frac{a_C}{a_{Fe}V} \propto \frac{a_C}{V} \tag{2-10}$$

which is a quantity per unit volume and therefore the atomic fraction can be used in the diffusion equation.

For an accurate value of the interface carbon concentration, carbon diffusion on the austenite domain has to be implemented. The boundaries of this domain are the interface with ferrite S and the boundary of the whole domain $\partial\Omega$. The diffusion coefficient is computed by

$$D(z) = D_0 \cdot e^{-\frac{Q(z)^{\gamma}}{RT}}, \tag{2-11}$$

where D_0 and Q^γ respectively are the pre-exponential constant and the activation energy for carbon diffusion. It is assumed that the activation energy may be different at grain interfaces. As stated, remind that D does not depend on the carbon concentration x, only on the location in the domain.

Recall the two boundary conditions on $\partial\Omega^\gamma$, as shown below.

$$
\begin{cases}
\frac{\partial x}{\partial n} &= 0 & \text{on } \partial\Omega \\
\frac{\partial x}{\partial n} &= -(x_s^\gamma - x^\alpha)v_n & \text{on } S
\end{cases}
$$

The non-zero Neumann boundary condition is important when cells transform. Whenever this happens, the excess carbon x^e of a newly transformed cell that corresponds with the term $(x_s^\gamma - x^\alpha)$ is instantaneously distributed over neighbouring austenite cells. Furthermore, assume that no cells transform between t_0 and $t_0 + \Delta t$, i.e Ω^γ is constant and on $[t_0, t_0 + \Delta t]$. Using this approach, the boundary conditions for the diffusion equation reduce to zero-Neumann conditions on the whole boundary $\partial\Omega^\gamma$ and the diffusion problem can be stated as:

Find $x(t_0 + \Delta t)$ on $\Omega^\gamma(t)$ such that

$$
\begin{cases}
\frac{\partial x}{\partial t} &= \nabla \cdot (D(z)\nabla x) & \text{in } \Omega^\gamma(t), \quad t_0 < t \leq t_0 + \Delta t \\
\frac{\partial x}{\partial n} &= 0 & \text{on } \partial\Omega^\gamma(t)
\end{cases},
$$

given $x(t_0)$ on Ω^γ and $D(z)$ on Ω.

Chapter 3

Methods

3-1 Smoothed Carbon Interface Concentration

When computing the growth velocity v_n for a ferrite interface cell, a value for the carbon interface concentration at this cell x_s is required. This interface concentration is determined in two steps. For all neighbouring austenite interface cells a non-trivial value for the carbon concentration is defined. The carbon interface concentration x_s^i of ferrite interface cell i is computed as

$$x_s^i = \frac{\sum\limits_{j \in \mathcal{M}_i} w_{ji} x_j}{\sum\limits_{j \in \mathcal{M}_i} w_{ji}}, \tag{3-1}$$

where the weights w_j are defined as

$$w_{ji} = \begin{cases} 0 & \text{cell } j \text{ is ferrite ,} \\ 1 & \text{cells } i \text{ and } j \text{ are 1-nearest neighbours and cell } j \text{ is austenite,} \\ \frac{1}{\sqrt{2}} & \text{cells } i \text{ and } j \text{ are 2-nearest neighbours and cell } j \text{ is austenite,} \\ \frac{1}{\sqrt{3}} & \text{cells } i \text{ and } j \text{ are 3-nearest neighbours and cell } j \text{ is austenite.} \end{cases} \tag{3-2}$$

The definition of the Moore neighborhood $\mathcal{M}_i$ of cell i and k-nearest neighbours are defined in Equation (2-5) and Table 2-1.

An attempt is made to reduce interface instabilities due to numerically introduced errors by smoothing the interface concentrations. Based on the level s of smoothing, the interface carbon concentration is averaged over the $(2s + 1) \times (2s + 1)$-cells around the reference cell. The smoothed carbon interface concentration of level $s = 1$ $\tilde{x}_s^i$ at reference cell i is computed as

$$\tilde{x}_s^i = \frac{\sum\limits_{j \in \mathcal{M}_i} w_{ji} x_s^i}{\sum\limits_{j \in \mathcal{M}_i} w_{ji}}, \tag{3-3}$$

where the weights w_j are defined as

$$w_{ji} = \begin{cases} 1 & \text{cell } j \text{ is ferrite interface} \\ 0 & \text{else} \end{cases}. \tag{3-4}$$

In general, the level s smoothed carbon interface concentration $\tilde{x}_s^i$ at reference cell i is defined as

$$\tilde{x}_s^i = \frac{\sum\limits_{j \in \mathcal{S}} x_s^i \mathbf{1}\{j \text{ is ferrite interface}\}}{\sum\limits_{j \in \mathcal{S}} \mathbf{1}\{j \text{ is ferrite interface}\}}, \tag{3-5}$$

where $\mathcal{S}$ are the indices of the $(n_s \times n_s)$ Moore neighbourhood of cell i and $\mathbf{1}\{\text{statement}\}$ is the indicator function defined as

$$\mathbf{1}\{\text{statement}\} = \begin{cases} 1 & \text{statement is true,} \\ 0 & \text{statement is false.} \end{cases} \tag{3-6}$$

Remark that for $\Delta z \to 0$ this method reduces to smoothing over a point, thus using the value of carbon concentration in that point. This behaviour is desirable in the sense that the solution of the discretized problem converges to the exact problem.

Inspiration   This method of carbon smoothing at the interface is based on an idea from Y. van Leeuwen[21]. To garantee interface stability, the idea was to use an infinite carbon diffusion coefficient at the interface. This results in a constant value for the interface concentration, i.e. a constant interface velocity across the whole interface.

3-2   Adaptive time steps

For this model the method of lines is used for time integration. This means that the nodes on which carbon concentration is computed, are fixed. However, at which points in time these values are computed may depend on the simulation itself. Schematically the method is given in Figure 3-1. The thick black vertical lines represent the set of points in time and space where the solution might be computed. The thin white interruptions in these lines represent an example of a possible outcome of points where the solution has been computed. The concept of adaptive time stepping is based on the combination of accuracy and efficiency. Large changes in the solution result in small time steps and small changes allow larger time steps. The time step Δt will be chosen in such a way that the event of 2-nearest and 3-nearest neighbours simultaneously tranforming due to one growing ferrite interface cell can not happen. Therefore, the time step is restricted such that the growth length of a cell does not change more than the difference in distance between a direct and a diagonal neighbor. The following time step criterion is the result,

$$\Delta t < (\sqrt{3} - \sqrt{2}) \cdot \frac{\Delta z}{v_{\max}}, \tag{3-7}$$

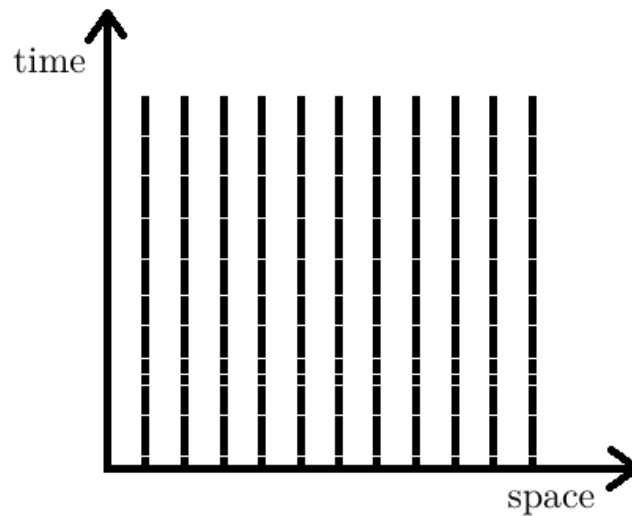where $v_{\max}$ is the maximum grain interface velocity.

Figure 3-1: Sketch of an example of the method of lines for time integration.

3-3   Interface Growth Methods

Outward Growth Method   A transformation method using the growth length ℓ is formulated Section 2-3. This approach can be interpreted from the perspective of growing cells, based on the question: Does the ferrite boundary cell expand? Using the Euler forward time integration method, the growth length ℓ after a time step of Δt is computed as

$$\ell(t + \Delta t) = \ell(t) + v\Delta t, \tag{3-8}$$

where the growth velocity is computed using the classical equation $v = M\Delta G$, as found in Bos et al.[8]. Whenever a ferrite cell has a growth length ℓ that exceeds the distance to a neighbouring cell, its neighbouring cell transforms. As initial growth length $\ell - \Delta z$ is used for consistency.

Inward Growth Method   A different approach is to change the perspective towards the austenite interface cells: Does the austenite boundary cell transform? This results in a more sophisticated strategy that also takes the amount of growing neighbouring ferrite cells into account. As an intuitive support for this approach, it does make sense that a cell will transform earlier if there is interface growth coming from multiple directions instead of only one. The latter approach assigns a percentage of transformation to the austenite interface cells.

The inward growth λ, defined for all austenite interface cells, is introduced here. The inward growth is defined as

$$\lambda_i = \sum_{j \in \mathcal{M}_i} w_{ji}\ell_j, \tag{3-9}$$

$$w_{ji} = \begin{cases} 1 & \text{cells } i \text{ and } j \text{ are 1-nearest neighbours,} \\ \frac{1}{\sqrt{2}} & \text{cells } i \text{ and } j \text{ are 2-nearest neighbours,} \\ \frac{1}{\sqrt{3}} & \text{cells } i \text{ and } j \text{ are 3-nearest neighbours,} \end{cases} \tag{3-10}$$

where w_{ji} are weights and ℓ_j is the growth length. The definition of the Moore neighborhood $\mathcal{M}_i$ of cell i and k-nearest neighbours are presented in Equation (2-5) and Table 2-1. Austenite interface cell i transforms if $\lambda_i > \theta\Delta z$, where Δz is the grid spacing. The value of θ can be computed using the condition that a straight interface with a constant velocity v_c should move accordingly. Consider a straight vertical interface in $\mathbb{R}^2$, see Figure 3-2, moving with a velocity of $v_c > 0$. Let $\ell_1 = \ell_2 = \ell_3 = \ell$. Then λ is computed as
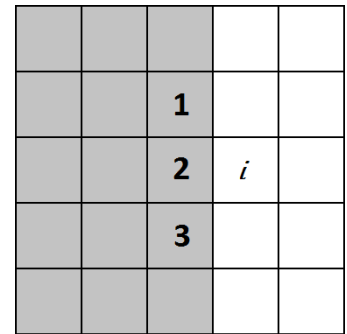

$$\begin{aligned} \lambda_i &= \tfrac{1}{\sqrt{2}}\ell_1 + \ell_2 + \tfrac{1}{\sqrt{2}}\ell_3 \\ &= \tfrac{2}{\sqrt{2}}\ell + \ell \\ &= (1 + \sqrt{2})\ell. \end{aligned} \tag{3-11}$$

Figure 3-2: Derivation of θ.

The transformation occurs when $\ell > \Delta z$. It follows that $\frac{\lambda_i}{1+\sqrt{2}} > \Delta z \Leftrightarrow \lambda_i > (1 + \sqrt{2})\Delta z$. Hence, $\theta = 1 + \sqrt{2}$ in the 2-dimensional case. For three dimensions the value of θ can be

found analogously,

$$
\begin{aligned}
\lambda &= 4 \cdot \tfrac{1}{\sqrt{2}}\ell + 4 \cdot \tfrac{1}{\sqrt{3}}\ell + \ell \\
&= \tfrac{2}{\sqrt{2}}\ell + \ell \\
&= (1 + 2\sqrt{2} + \tfrac{4}{3}\sqrt{3})\ell.
\end{aligned}
\tag{3-12}
$$

Therefore, in a three dimensional cellular automaton $\theta = 1 + 2\sqrt{2} + \tfrac{4}{3}\sqrt{3}$. Transformation of the austenite cell occurs when $\lambda > \theta \Delta z$. The initial growth length of the cell is set at $\tfrac{\lambda}{\theta} - \Delta z$ for consistency.

3-4 Carbon diffusion

The introduced method of smoothing interface carbon concentration can be seen as a method to bypass the use of a higher diffusion coefficient at the ferrite-austenite interface. From an experimental point of view it is acceptable to say that diffusion of carbon atoms at grain interfaces actually is faster. Therefore, the diffusion coefficient D could be a function depending on space.

$$
D(z) = \begin{cases}
D_0 \cdot \exp\left(\dfrac{Q_d^{\gamma}}{RT}\right) & \text{for } z \in \Omega^{\gamma}, \\[2mm]
D_0 \cdot \exp\left(\dfrac{Q_d^{\alpha,\gamma}}{RT}\right) & \text{for } z \in \partial\Omega^{\gamma} \cap \partial\Omega^{\alpha}, \\[2mm]
D_0 \cdot \exp\left(\dfrac{Q_d^{\gamma,\gamma}}{RT}\right) & \text{for } z \in \partial\Omega^{\gamma} \setminus \partial\Omega^{\alpha}.
\end{cases}
\tag{3-13}
$$

Note that the diffusion coefficient is locally a constant. The carbon diffusion problem is stated in the model section as: Find $x(t_0 + \Delta t)$ on $\Omega^{\gamma}(t)$ such that

$$
\begin{cases}
\dfrac{\partial x}{\partial t} = \nabla \cdot (D(z)\nabla x) & \text{in } \Omega^{\gamma}(t), \qquad t_0 < t \leq t_0 + \Delta t, \\[2mm]
\dfrac{\partial x}{\partial n} = 0 & \text{on } \partial\Omega^{\gamma}(t).
\end{cases}
\tag{3-14}
$$

To solve this time step for the diffusion equation, use implicit Euler time integration in combination with finite differences. For every cell the carbon concentration is approximated by x_i. The main reason to apply an implicit method is its property of unconditional stability which allows larger time steps[22]. Implementing this method yields

$$
\frac{x_i^{k+1} - x_i^k}{\Delta t} = \frac{D_i}{(\Delta z)^2}\left(x_{i-1}^{k+1} + x_{i+1}^{k+1} + x_{i-n}^{k+1} + x_{i+n}^{k+1} - 4x_i^{k+1}\right).
\tag{3-15}
$$

This expression is rewritten as the matrix equation

$$
Ax^{k+1} = x^k,
\tag{3-16}
$$

where $A = I - T$ is a sparse symmetric positive definite matrix. Using the Kronecker product $\otimes$, the matrix T is constructed in three steps:

1. Compute

$$T = \frac{D\Delta t}{(\Delta z)^2}(S \otimes I + I \otimes S), \tag{3-17}$$

where I is the identity matrix of dimension $n_z \times n_z$ and S has the structure

$$S = \begin{bmatrix} -1 & 1 & & & \\ 1 & -2 & 1 & & \\ & \ddots & \ddots & \ddots & \\ & & 1 & -2 & 1 \\ & & & 1 & -1 \end{bmatrix}. \tag{3-18}$$

2. Set all rows and columns corresponding to ferrite cells to zero. (The carbon concentration does not change in ferrite, thus all ferrite rows are set to zero. Also, due to zero-flux boundary conditions the ferrite columns are set to zero.)

3. Set the diagonal entries equal to minus the row sum that excludes the diagonal value, due to zero-flux boundary condition between austenite-ferrite, i.e.

$$T_{ii} = -\sum_{j \neq i} T_{ij}. \tag{3-19}$$

CG method   The implicit Euler time integration method includes solving a linear system. In our case, from numerical analysis it is known that by applying finite differences on the diffusion equation with zero-flux boundary conditions, the resulting matrix is a sparse symmetric positive definite matrix. An effective way to solve this type of linear system is to apply the Conjugate Gradient (CG) method. The CG method is an iterative method for solving large sparse linear systems, first published in 1952 by Hestenes and Stiefel[23].

3-4-1   The algorithm

For every iteration in time, the algorithm consists of the following steps.

1. Compute the interface carbon concentration for the ferrite interface cells. This is necessary to compute the interface velocity during the next time step. It takes two steps to compute x_s. For ferrite interface cell i, compute x_s by the weighted average of carbon concentration of its austenite neighbours. Then, smoothe x_s by taking the average x_s inside the $n_s \times n_s$ cell square around cell i, see the carbon interface smoothing section.

2. Compute v for all relevant cells, using the classical equation $v = M \Delta G$. The driving force ΔG is assumed to be a function of the temperature T and the carbon interface concentration x_s. Using the software Thermo-Calc® this function can be extracted for the desired steel alloy.

3. Compute ℓ for all relevant cells, using Euler forward time integration: $\ell(t + \Delta t) = \ell(t) + v \Delta t$.

4. Compute λ for all relevant cells, by taking the weighted sum over its direct and diagonal neighbours.

5. Transform all cells according to outward growth length or inward growth. The outward growth method can be found in the literature[8], the inward growth method is based on an implementation on a hexagonal grid[9].

   - **Outward growth method:** Consider the ferrite interface cells. If the growth length of cell i reaches one of its neighbours, its neighbouring austenite cells will transform into ferrite. The time stepping will be chosen in such a way that it is not possible that 1-nearest, 2-nearest and diagonal neighbours of a ferrite interface cell will transform simultaneously.

   - **Inward growth method:** Consider the austenite interface cells. If the inward growth of cell i exceeds $(1 + 2\sqrt{2} + \frac{4}{3}\sqrt{3})\Delta z$, then cell i transforms into ferrite.

6. Redistribute the excess carbon from newly transformed cells. If cell i transforms, the carbon amount will be set at x^α. The remaining carbon will be distributed to its austenite neighbours, optionally weighted or not according to distance.

7. Solve the diffusion equation for the carbon concentration on the austenite part of the domain, using Neumann boundary conditions on the interface between austenite and ferrite and on the boundary of our square domain Ω.

Chapter 4

Results

Discrete or continuous interface? The movement of the interface between austenite and ferrite depends partly on the carbon concentration at the interface. Since the carbon diffusivity in ferrite is large in comparison to austenite, it is assumed that the carbon concentration in ferrite instantaneously attains its equilibrium value. The carbon concentration in austenite is determined by solving the diffusion equation on the austenite part of the domain. Using a CA model, the austenite domain does not change continuously, but with jumps every time a cell is transformed. Consider a cell that transforms during time step iteration k, i.e. at time step k it belongs to austenite and at time step $k+1$ it belongs to ferrite. The excess carbon $x_k - x^\alpha$ then flows instantaneously towards its neighbouring cells. After this redistribution of carbon, a time step for the diffusion equation is applied on the austenite domain. Using this approach, it is possible to exceed the equilibrium concentration of carbon in austenite. This is physically impossible. Therefore, it is necessary to investigate if the CA approach where the interface is restricted to fixed cells can be justified. It would be desirable to observe that the fixed grid method behaves similar to an adaptive grid method such as the Murray-Landis method[24].

How can unstable interface growth be controlled? As found in other literature[9], the interface between ferrite and austenite is not always stable. According to observable physics, dendritic growth does not happen when ferrite grows in austenite. For the interface mobility large in comparison with the diffusion coefficient, i.e. $M \gg D$, it seems that interface instabilities[25] are unavoidable. Due to discretization into square cells in combination with a freedom restriction on the interface position, a perturbation error is easily introduced. A small perturbation error of carbon concentration will cause perfect spherical growth to evolve into dendritic growth. If an erroneous carbon accumulation area is formed, the interface shape will not recover from the error. When observing the steel micro structure after real experiments, dendritic growth does not seem realistic. The main causes for dendritic growth behaviour are assumed to be the discretized square grid and the absence of surface tension in the model. However, incorporating surface tension in a grain growth model would complexify the model and drastically increase computation times. Also, the influence of surface tension

on the growth kinetics is small. Is it the right way to go to add physical phenomena to reduce numerical error issues? Using curvature in a CA model has been done by Janssens[3], which he summarized by his conclusion: *as grains get large relative to the cell size, the grain boundary curvature decreases relative to the cell size, and consequently the cellular automaton underestimates the driving pressure.* Another model with curvature incorporated can be found in Raghavan[16]. In a paper of Lan[9] a different grid is used in order to reduce instabilities. Using a hexagonal grid reduces instabilities, but it did not eliminate the grid anistotropy. It can be stated that there is no golden rule yet to fully avoid unstable interface growth.

4-1   Comparison: CA to Murray-Landis

The main point of interest in the transformation model is the austenite ferrite interface $S(t)$, which is equivalent to the fraction ferrite $f_\alpha(t)$ for a 1-dimensional model. The cellular automaton approach is a discrete method in space. Therefore, the transformation process results in interface jumps from node to node as time passes. The same happens to the carbon concentration that is pushed forward in front of the interface. The unphysical phenomenon that occurs in the model is then an over-saturated part of the austenite domain. Another continuous approach in $\mathbb{R}^1$ is the *Murray-Landis* method for concentration based moving boundary problems. This method has a dynamic grid that is updated every time step. The interface is not restricted to a pre-defined grid, but is allowed to lie anywhere in the domain. The carbon concentration can not exceed the physical upper limit in this case.
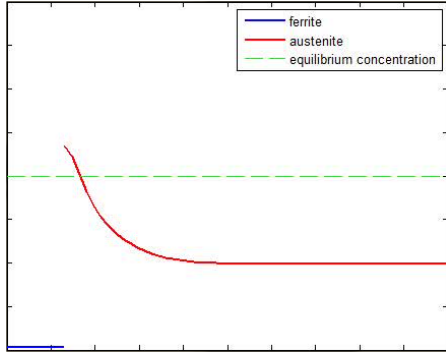

Figure 4-1: The 'overshoot' of carbon concentration in cellular automaton.
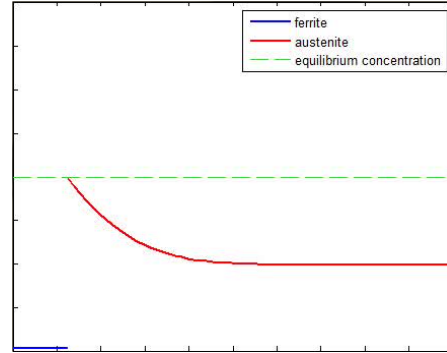

Figure 4-2: The realistic carbon concentration profile of the continuous Murray-Landis method.

It is desired to show that the two methods are equivalent for $\Delta z \to 0$. The time step Δt is coupled to the space increment dz for stability, $\Delta t = 0.9 \cdot \frac{\Delta z}{v_{\max}}$, where $v_{\max}$ is determined from a previous simulation using the same parameters. Let us denote the fraction of ferrite according to the CA method and the Murray-Landis method as f_1 and f_2 respectively. Then, the error is defined as $e = ||f_1 - f_2||_\infty$, using the maximum norm of the difference between the two methods. The infinity norm is used because this norm is independent of the number of grid points. Hence, the task is to show that $e \to 0$ as $\Delta z \to 0$.

For a decreasing sequence of space increments Δz and according sequence of time increments Δt, the error $e = ||f_1 - f_2||_\infty$ was computed. Using a fixed grid, the interface $S(t)$ is restricted

to values on the grid. Therefore, an error due to grid spacing is tolerated and expected to occur. Figure 2-4 shows the results of this sequence of simulations, using logarithmic scaling on both axes.
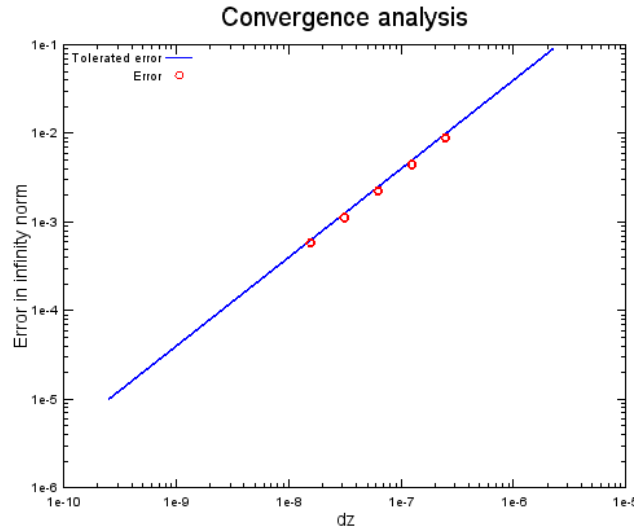

Figure 4-3: Experimental convergence

Analyzing the slope of the errors, an experimental order of convergence of 1 is obtained. The conclusion that the fixed grid method converges linearly to the adaptive grid method can be drawn from this. An error up to the grid spacing is tolerated in the CA method, due to the restriction that $S(t)$ has to lie on a node. Furthermore, observe that the error is smaller than the tolerated error due to grid spacing for any Δz tested. In conclusion, it can be stated that the fixed grid method is accurate up to an error induced by the grid spacing.

The convergence analysis has been performed using the parameters in Table 4-1. Also, the excess length $\ell_i - \Delta z$ should be set as the initial length of a newly transformed cell.

Description	Variable	Value	Unit
Length of interval	L	25e-6	m
Simulation time	t_f	600	s
Temperature	T	1000	K
Gas constant	R	8.314462	J K^{-1}mol^{-1}
Pre-exponential diffusion factor	D_0	0.15e-4	m^2 s^{-1}
Pre-exponential mobility factor	M_0	0.035	m J^{-1} s^{-1}
Activation energy for carbon diffusion	Q_D^γ	142e3	J mol^{-1}
Activation energy for ferrite recrystallization	$Q^{\alpha\gamma}$	140e3	J mol^{-1}
Average carbon concentration	x_0	4.1580e-3	atomic fraction

Table 4-1: Parameter Values: Convergence Analysis

4-2   Inward Growth Method

For increasing values of interface mobility M_0, the transformation rules of outward and inward growth are compared using identical input parameters on a 100×100 grid. No interface carbon smoothing has been applied in these simulations.

Low Mobility   First, the two methods using a low value for the interface mobility are compared. The outward growth method does not show dendritic growth. However, the grain shape did not grow into a circle, but a polygon. This behaviour is analyzed in a paper writ-

Figure 4-4: *Outward growth (l) and inward growth (r):* $M_0 = 0.1$, $t_f = 20$

ter by Marek[11] and is acceptable as an approximation of a circle. When analyzing the output of the inward growth method, a circular shape is can be observed. The growth behaviour is symmetric on the square grid in this case and thus more realistic. After a 20 second simulation, the grain diameter is around $7 \mu m$.
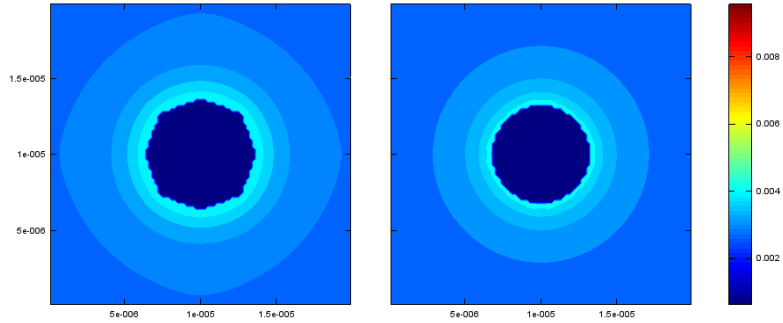
Medium Mobility   Let us now consider a higher interface mobility which causes interface instability. The outward growth method shows clear accumulation areas of carbon, resulting in dendritic *fingers* that grow faster in the direction of the least carbon concentra-

Figure 4-5: *Outward growth (l) and inward growth (r):* $M_0 = 0.6$, $t_f = 10$

tion. When examining the results of the same test using the inward growth method, significant decrease of dendritic growth is seen. In fact, the grain shape has a realistic circle shape. After a 10 second simulation, the grain diameter is around $10 \mu m$.
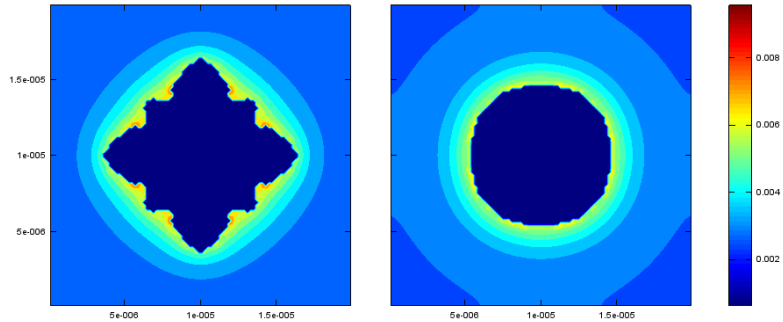
High Mobility The limits of the inward growth method are investigated. When increasing the interface mobility even further, the point is reached where also the behaviour of this method is unsatisfactory. Although one could argue that the grain shape from the inward

Figure 4-6: *Outward growth (l) and inward growth (r):* $M_0 = 1.5$, $t_f = 10$

growth method is 'better', it is not the desired circular shape. Thus, also this method has its limits. After a 10 second simulation, the grain diameter is around $14\mu m$.

4-3 Carbon Interface Smoothing

For increasing values of interface mobility M_0, the effectiveness of carbon interface smoothing is tested on a 100×100 grid. The inward growth method is used in these simulations. For the domain a square with length $L = 20\mu m$ is used.

Low Mobility (Figure 4-7) For a low interface mobility there is not much to improve. Minor but no significant differences can be found in the isoconcentration lines, but the grain shape seems identical. After a 20 second simulation, the grain diameter is around $6\mu m$.

Medium Mobility (Figure 4-8) For a higher interface mobility there is more space for improvements. The interface behaves less wild when the smoothing area is enlarged. The grain shape approximates the circle better when applying the carbon interface smoothing method. It seems that the smoothing has an effect on the interface stability, but is unable to remove the interface instabilities completely. After a 10 second simulation, the grain diameter is around $9\mu m$.

High Mobility (Figure 4-9) When simulating a more extreme case, the same improvements as from less extreme values for interface mobility are observed. The dendritic graing growth is reduced, but the method by itself is unable to avoid dendritic grain growth. After a 10 second simulation, the grain diameter is around $15\mu m$.
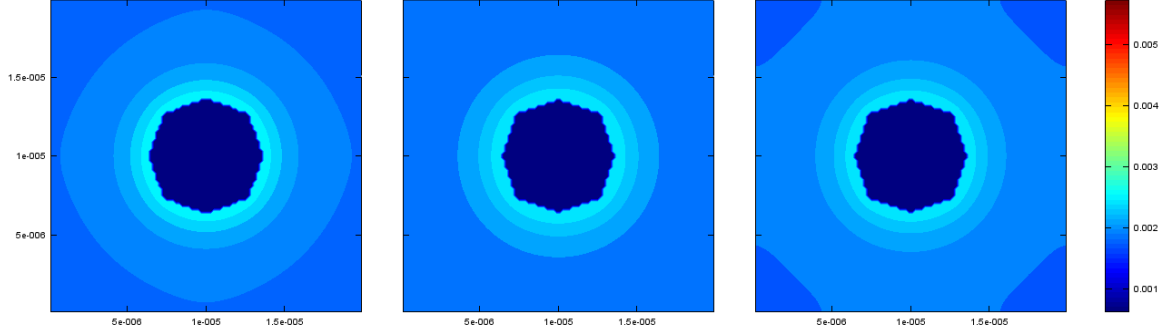
Figure 4-7: *No smoothe(l),* 3×3-*smoothe(m) and* 5×5-*smoothe(r):* $M_0 = 0.1$, $t_f = 20$

Figure 4-8: *No smoothe(l),* 3×3-*smoothe(m) and* 5×5-*smoothe(r):* $M_0 = 0.6$, $t_f = 10$

Figure 4-9: *No smoothe(l),* 3×3-*smoothe(m) and* 5×5-*smoothe(r):* $M_0 = 1.5$, $t_f = 10$

4-4 Stabilizing methods combined

Both improvements on literature models reduce interface instabilities and are unable to eradicate the problem. Therefore, by combining both methods, it is only expected to further reduce dendritic grain growth, not eliminate. A large analyisis of different cases can be done, but this is skipped because results seem obvious when starting at the most extreme test case. Combining the inward growth method with the carbon smoothing method of level s, IG&CS(s), the following plots are given as a result. After a 10 second simulation, the grain diameter is around $12\mu m$.
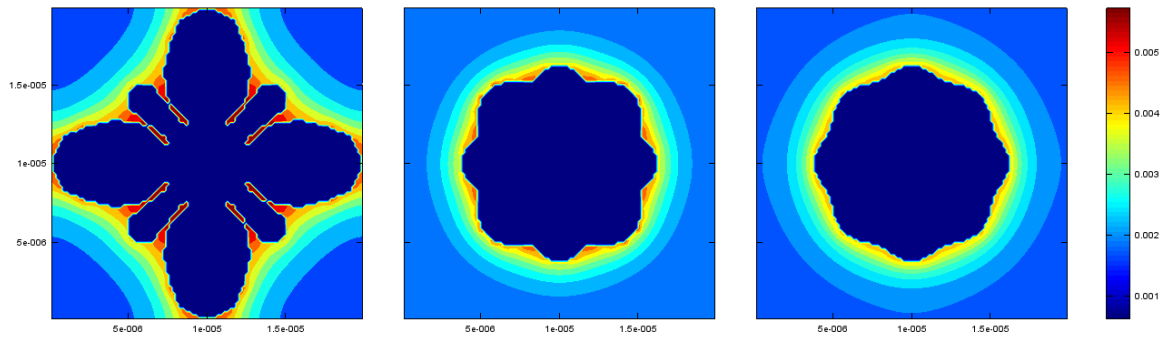

Figure 4-10: OG&CS(0)(left), IG&CS(1)(middle) and IG&CS(2)(right)

Parameters and Initial State

For all results the parameter values from Table 4-2 have been used. The initial grain shape used was a small thick cross, depicted in Figure 4-11. A grid size of 100×100 cells has been used. For low interface mobility values, the simulations have been extended from 10 to 20 seconds. This has been done to increase grain size and therefore visibility of the results.
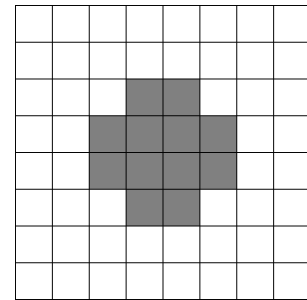

Figure 4-11: The initial ferrite grain shape.

Description	Variable	Value	Unit
Length of interval	L	20e-6	m
Simulation time	t_f	10 or 20	s
Temperature	T	1000	K
Gas constant	R	8.314462	J K^{-1}mol^{-1}
Pre-exponential diffusion factor	D_0	0.15e-4	m^2 s^{-1}
Pre-exponential mobility factor	M_0	0.1, 0.6 or 1.5	m J^{-1} s^{-1}
Activation energy for carbon diffusion	Q_D^γ	142e3	J mol^{-1}
Activation energy for ferrite recrystallization	$Q^{\alpha\gamma}$	140e3	J mol^{-1}
Average carbon concentration	x_0	4.1580e-3	atomic fraction

Table 4-2: Parameter Values: Testing Stability Methods

4-5 Fast Interface Diffusion

Since the carbon smoothing method relates to higher interface diffusion, a higher interface diffusion coefficient at the ferrite interface is used in these tests. From Equation (3-13) in Section 3-4, the diffusion coefficient at the ferrite austenite interface is assumed to be

Figure 4-12: Region of higher diffusion coefficient around the grain in $\mathbb{R}^2$ is coloured grey.

$$D(z) = D_0 \cdot \exp\left(\frac{Q_d^{\alpha,\gamma}}{RT}\right),$$

where $Q_d^{\alpha,\gamma} = \rho Q_d^{\gamma}$ is the activation energy in austenite multiplied by some factor ρ. First, the results of a stable test case in $\mathbb{R}^3$ will be shown. Then, results of an unstable test case are presented and attempted to improve by lowering ρ. These tests are performed under the exact same circumstances, except the factor ρ which is varied. For $M = 0.1$ the resulting grain has a close to spherical shape, see Fig 4-13.
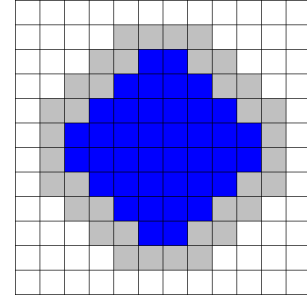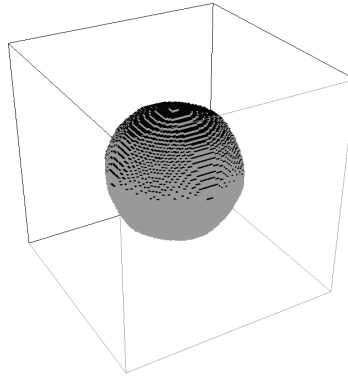

Figure 4-13: Spherically shaped ferrite grain.

Now, proceeding to an extreme case for $M = 0.5$, the resulting grain shape is a dendrite, see Fig 4-14, 4-15 and 4-16. This dendritic growth is attempted to reduce by decreasing the factor ρ. Without higher interface diffusion $\rho = 1$ and the grain shape is unsatisfactory. When lowering the factor to $\rho = 0.9$, the grain shape is improved but still not acceptable. The last test shows that for $\rho = 0.8$ the grain shape is very similar to a sphere which is desired. The simulations all end when the ferrite fraction exceeds 8.5%.
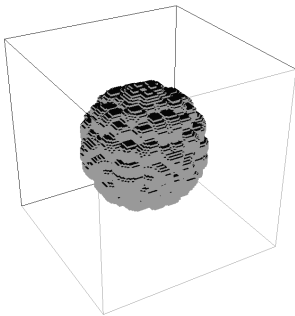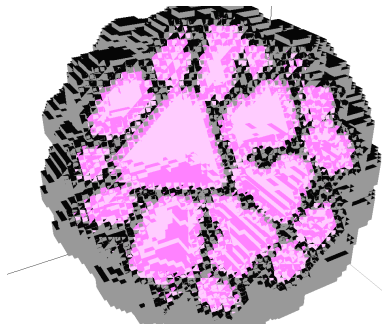
Figure 4-14: A wobbly shape from the outside.

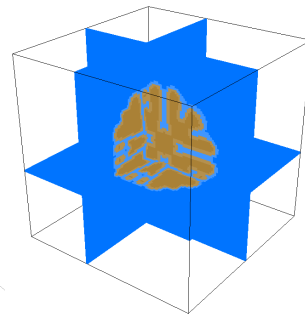**Figure 4-15:** A look from the inside reveals the dendritic structure.
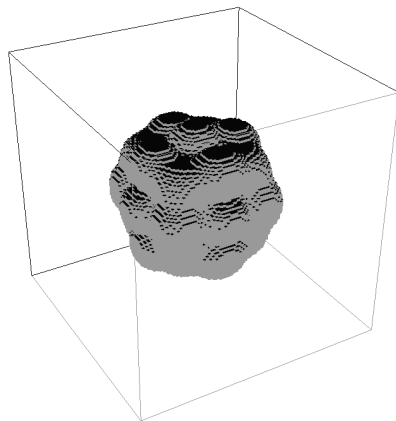
Figure 4-16: Slices of the grain.

Figure 4-17: Outer grain view, $\rho = 0.9$.

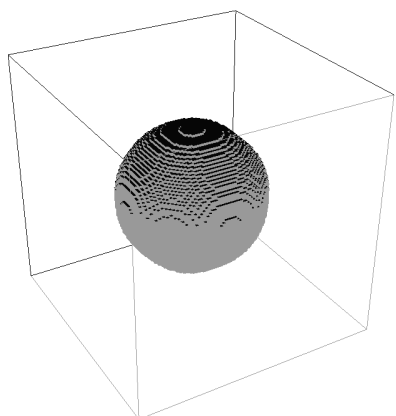**Figure 4-18:** Inner grain view, $\rho = 0.9$.

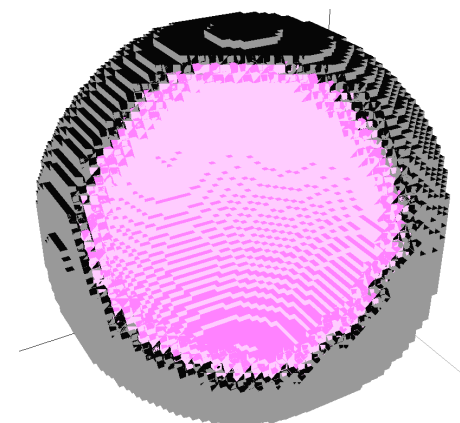**Figure 4-19:** Outer grain view, $\rho = 0.8$.

Figure 4-20: Inner grain view, $\rho = 0.8$.

The parameters used in this simulation can be found in Table 4-3

Description	Variable	Value	Unit
Length of interval	L	20e-6	m
Temperature	T	1000	K
Gas constant	R	8.314462	J K^{-1}mol^{-1}
Pre-exponential diffusion factor	D_0	0.15e-4	m^2 s^{-1}
Pre-exponential mobility factor	M_0	0.1, 0.5	m J^{-1} s^{-1}
Activation energy for carbon diffusion	Q_D^{γ}	142e3	J mol^{-1}
Activation energy for ferrite recrystallization	$Q^{\alpha\gamma}$	140e3	J mol^{-1}
Average carbon concentration	x_0	5.584e-3	atomic fraction

Table 4-3: Parameter Values: Increased interface diffusion

4-6   Fraction Curves

Dilatometric experiments[20] are able to give information of ferrite fraction curves during transformation. For a specific type of steel, a fraction curve of austenite cooled at 600 °C is approached by the model in $\mathbb{R}^3$. In Figure 4-21 the development of ferrite grains are visible in slices of the domain. The time intervals between the images are not all the same, just chronological. Austenite grains are coloured orange and ferrite grains are coloured blue.
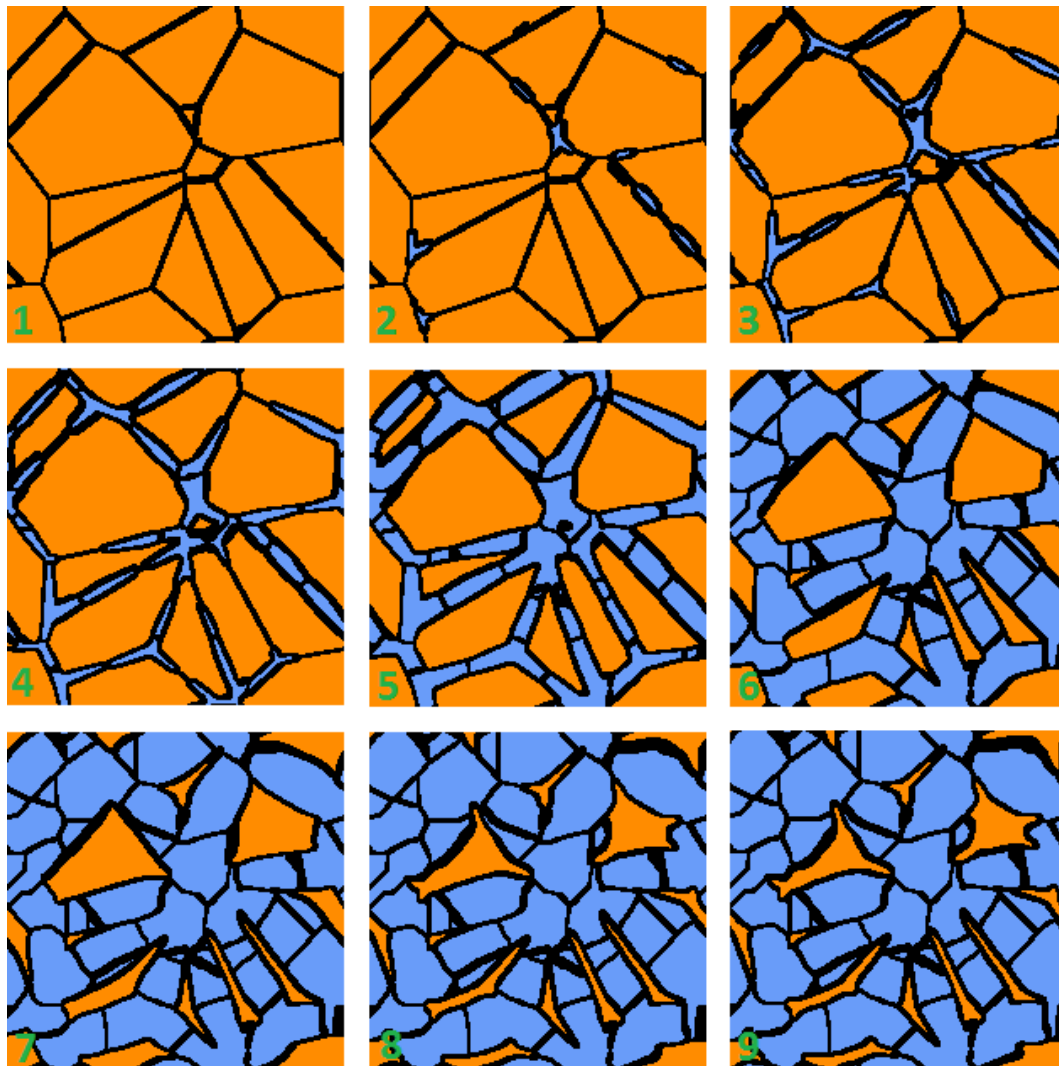

Figure 4-21: The growth of ferrite inside austenite.

The final microstructure is visualized in Figure 4-22 and 4-23. Observe that dendrites are not present in this structure.

Figure 4-22: Resulting austenite ferrite structure.

Figure 4-23: Resulting internal grain structure.

The fraction curve is plotted in Figure 4-24. It can be observed that initially the transformation follows the experimental data. After 10 seconds of simulation the model predicts a too fast transformation. At the end, the model seems to overpredict the ferrite fraction by about 8%.

Figure 4-24: The modeled fraction curve and the experimental fraction curve.

The parameters used in this simulation can be found in Table 4-4

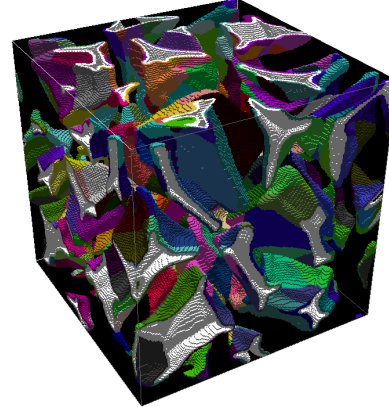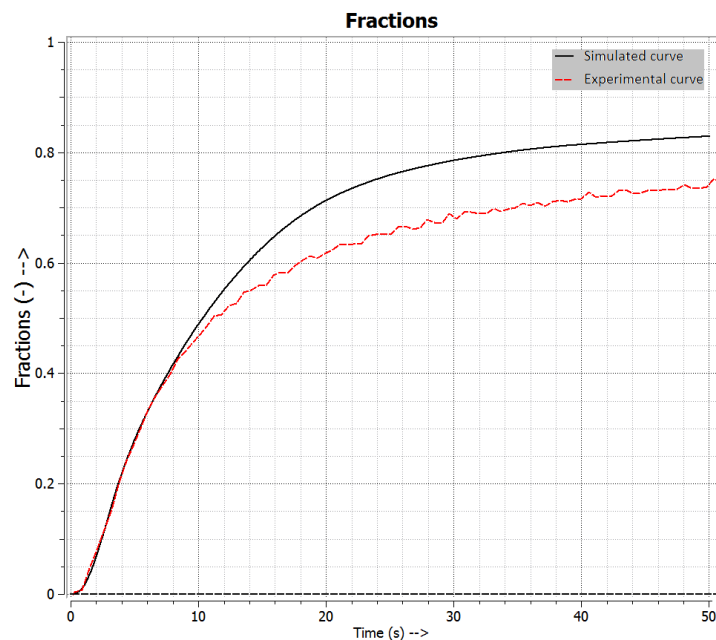| Description	Variable	Value	Unit
Cube dimension	L	20e-6	m
Temperature	T	873.15	K
Gas constant	R	8.314462	J K^{-1}mol^{-1}
Pre-exponential diffusion factor	D_0	0.15e-4	m^2 s^{-1}
Pre-exponential mobility factor	M_0	0.05	m J^{-1} s^{-1}
Activation energy for carbon diffusion	Q_D^γ	142e3	J mol^{-1}
Activation energy for ferrite recrystallization	$Q^{\alpha\gamma}$	140e3	J mol^{-1}
Average carbon concentration	x_0	5.584e-3	atomic fraction
Initial austenite grain density		5.0e14	m^{-3}
Number of ferrite nucleations		2.225e15	m^{-3}
Fast grain boundary growth factor		0.85	
Fast interface diffusion factor	ρ	0.75	

Table 4-4: Parameter Values: Ferrite fraction curve

Chapter 5

Discussion

The comparison of the cellular automaton with the Murray-Landis method supports the use of cellular automaton for the austenite to ferrite transformation. The unphysical overshoot of carbon concentration does not create a problem and should not be worried about. However, one should take the excess growth length into account, also for the inward growth method. As a result, for smaller grid sizes the grain shape tends to an octagon. The strange phenomenon of a rather circular grain shape happens when ignoring the excess growth length on a medium sized grid. It seems perfectly fine, but according to the comparison the excess length should be implemented. Furthermore, when reducing the time step towards zero ignoring the excess growth length does not matter.

After a series of tests it became clear that the carbon smoothing method required a high level of smoothing in certain cases. This method resembles in some way a higher diffusion of carbon at the ferrite austenite interface. Therefore, applying a locally higher diffusion coefficient and disabling the smoothing method might be a good idea. On the other hand, discontinuities in the diffusion coefficient are bad for the condition of the problem. Probably this locally higher diffusion coefficient cannot be stretched too much.

Attempts have been made to incorporate a higher diffusion at interfaces between austenite grains themselves. Since essentially there is more opportunity for carbon atoms to jump around in the lattice, it does make sense. However, the width of the interface should not be determined by the grid spacing. The cell size is too large to approach interface thickness, therefore this does not seem to be a good idea to implement in the current structure.

Experiments have been done with a higher mobility on austenite austenite interfaces. However, determining the rate or factor for this parameter had to be mostly guessed. Also, the structures that develop during simulations should be realistic. How should this value be determined? Function fitting using derived data from experiments is perhaps a naive way.

The reduction of dendrites forming is clearly possible, but in specific cases it could still occur. But are these cases physically relevant? If not, further research should not be done in this direction anymore. The focus might shift to solving the more ill-conditioned problem of diffusion with a discontinuous diffusion coefficient on the domain.

Chapter 6

Conclusion

A 2-dimensional square grid cellular automaton for the austenite ferrite transformation has been reproduced based on literature. The model allows experimenting with the cellular automaton framework, making it possible to try different approaches for the subproblems. A 3-dimensional cubic grid cellular automaton for the austenite ferrite transformation has been made ready to use carbon diffusion without producing unphysical dendritic structures. The interface restriction that is a consequence of the Cellular Automata model has been analyzed by comparing the CA model with the Murray-Landis method which allows continuous interface movement. After carefully constructing the model, it has been shown that the 1-dimensional CA model does converge to the Murray-Landis solution as the grid spacing goes to zero. Furthermore, the causes of interface instabilities have been investigated. In the literature, transformation rules found are based on the outward growth. Even in stable cases, the grain shape tends to a octagon when applying the outward growth method. Changing the perspective to inward growth, a new transformation rule was found. This method works positive in two ways. Firstly, the stable case tends to a circular shape if one ignores overshoot in growth length. Secondly, dendritic grain growth is reduced and a higher value for interface mobility is allowed. In order to even further reduce instable interface growth, the carbon concentration at the interface was smoothed. Averaging the concentration over a couple of neighbouring cells, the numerically introduced errors in the concentration are spread to reduce impact on interface shape. As a result, this reduces dendritic growth even further. Instead of carbon smoothing, a higher diffusion coefficient at ferrite austenite interfaces is applied. For extreme cases of interface mobility, this method is able to tackle the problem of dendrites by raising the diffusion at the interface at the cost of a worse conditioned linear problem. Dendritic grain growth in cellular automaton could be history from now on. Using experimental dilatometry data, parameters of the model were adjusted to fit the fraction curve. Due to the many parameters, it is not easy to determine which are correct and which are wrong. Fast grain boundary growth, nucleation density, interface mobility and initial grain density are the four most important parameters. There are still tests necessary to determine these model parameters. The positive note on this simulation is that it is computed within a reasonable amount of time without dendritic grains.

Summary   A CA model for the austenite ferrite transformation has been significantly *improved*, the use of CA has been *justified* in some sense and the interface stability has been *improved*, eliminating the problem of unrealistic dendritic grains.

Research Questions   The major part of this thesis is about reducing interface instabilities and avoiding dendrites. However, it is known that surface tension also plays a small role in growth kinetics. *Could the implementation of surface tension in a cellular automaton completely avoid dendritic grain growth?* The current development in avoiding dendritic grain growth seems to be enough for the transformation simulations. *Are these new approaches enough?* How much should the interface be smoothed and how much higher should the interface diffusion really be? Definately these methods rise new questions. Also, with the higher interface diffusion resulting in a more ill-conditioned problem, the following question could become important. Is it possible to build a linear solver in parallel for higher efficiency? And what type of pre-conditioners are suited for this problem without changing the total amount of carbon in the system?

Bibliography

[1] C.-J. Huang, D. J. Browne, and S. McFadden, "A phase-field simulation of austenite to ferrite transformation kinetics in low carbon steels," *Acta materialia*, vol. 54, no. 1, pp. 11–21, 2006.

[2] E. J. Perez, *Numerical methods for vector Stefan models of solid-state alloys.* Ph. D. thesis, Delft University of Technology, 2006.

[3] K. Janssens, "An introductory review of cellular automata modeling of moving grain boundaries in polycrystalline materials," *Mathematics and Computers in Simulation*, vol. 80, no. 7, pp. 1361–1381, 2010.

[4] S. Raghavan and S. S. Sahay, "Modeling the topological features during grain growth by cellular automaton," *Computational Materials Science*, vol. 46, no. 1, pp. 92–99, 2009.

[5] C. Zheng and D. Raabe, "Interaction between recrystallization and phase transformation during intercritical annealing in a cold-rolled dual-phase steel: A cellular automaton model," *Acta Materialia*, vol. 61, no. 14, pp. 5504–5517, 2013.

[6] L. Zhang, Y. Wang, C. Zhang, S. Wang, and H. Ye, "A cellular automaton model of the transformation from austenite to ferrite in low carbon steels," *Modelling and Simulation in Materials Science and Engineering*, vol. 11, no. 5, p. 791, 2003.

[7] C. Bos and J. Sietsma, "A mixed-mode model for partitioning phase transformations," *Scripta Materialia*, vol. 57, no. 12, pp. 1085–1088, 2007.

[8] C. Bos, M. Mecozzi, and J. Sietsma, "A microstructure model for recrystallisation and phase transformation during the dual-phase steel annealing cycle," *Computational Materials Science*, vol. 48, no. 3, pp. 692–699, 2010.

[9] Y. Lan, D. Li, and Y. Li, "Modeling austenite decomposition into ferrite at different cooling rate in low-carbon steel with cellular automaton method," *Acta Materialia*, vol. 52, no. 6, pp. 1721–1729, 2004.

[10] Y. Lan, D. Li, and Y. Li, "A mesoscale cellular automaton model for curvature-driven grain growth," *Metallurgical and materials transactions B*, vol. 37, no. 1, pp. 119–129, 2006.

[11] M. Marek, "Grid anisotropy reduction for simulation of growth processes with cellular automaton," *Physica D: Nonlinear Phenomena*, vol. 253, pp. 73–84, 2013.

[12] D. An, S. Pan, L. Huang, T. Dai, B. Krakauer, and M. Zhu, "Modeling of ferrite-austenite phase transformation using a cellular automaton model," *ISIJ International*, vol. 54, no. 2, pp. 422–429, 2014.

[13] B. Zhu, Y. Zhang, C. Wang, P. X. Liu, W. K. Liang, and J. Li, "Modeling of the austenitization of ultra-high strength steel with cellular automation method," *Metallurgical and Materials Transactions A*, vol. 45, no. 7, pp. 3161–3171, 2014.

[14] M. Mecozzi, "Phase field modelling of the austenite to ferrite transformation in steels," 2006.

[15] J. Ågren, "A revised expression for the diffusivity of carbon in binary fe- c austenite," *Scripta metallurgica*, vol. 20, no. 11, pp. 1507–1510, 1986.

[16] S. Raghavan and S. S. Sahay, "Modeling the grain growth kinetics by cellular automaton," *Materials Science and Engineering: A*, vol. 445, pp. 203–209, 2007.

[17] B. Yang, L. Chuzhoy, and M. Johnson, "Modeling of reaustenitization of hypoeutectoid steels with cellular automaton method," *Computational Materials Science*, vol. 41, no. 2, pp. 186–194, 2007.

[18] D. Raabe, "Computational materials science the simulation of materials microstructures and properties wiley," 1998.

[19] S. Van Bohemen, C. Bos, and J. Sietsma, "Simulation of ferrite formation in fe-c alloys based on a three-dimensional mixed-mode transformation model," *Metallurgical and Materials Transactions A*, vol. 42, no. 9, pp. 2609–2618, 2011.

[20] T. A. Kop, "A dilatometric study of the austenite/ferrite interface mobility," 2000.

[21] Y. van Leeuwen, "Moving interfaces in low-carbon steel-a phase transformation model," 2000.

[22] J. van Kan, A. Segal, and F. Vermolen, *Numerical methods in scientific computing.* VSSD, 2005.

[23] M. R. Hestenes and E. Stiefel, *Methods of conjugate gradients for solving linear systems*, vol. 49. National Bureau of Standards Washington, DC, 1952.

[24] W. D. Murray and F. Landis, "Numerical and machine solutions of transient heat-conduction problems involving melting or freezing," *J. Heat Transfer*, vol. 81, pp. 106–112, 1959.

[25] W. W. Mullins and R. Sekerka, "Stability of a planar interface during solidification of a dilute binary alloy," *Journal of applied physics*, vol. 35, no. 2, pp. 444–451, 1964.